DEFENCE
SCIENCE & TECHNOLOGY

Sperm Whale Impulse Noise and Incoherent Narrowband CFAR Processing

Derek Bertilone and
Damien Killeen

DSTO-TR-1357

DEFENCE
SCIENCE & TECHNOLOGY

Sperm Whale Impulse Noise and Incoherent Narrowband CFAR Processing

Derek Bertilone and Damien Killeen

Maritime Operations Division
Systems Sciences Laboratory

DSTO-TR-1357

ABSTRACT

Impulsive noise interference of a biological origin is common in underwater acoustic environments. Here we report on properties of impulsive noise produced by sperm whales, recorded in deep water off the coast of Manus Island. We analyse the noise as a function of frequency band, and find strong non-Gaussian effects in the range 1-6 kHz. Sonar performance can be improved by utilising nonlinear filtering techniques from non-Gaussian detection theory. We demonstrate this by measuring empirical gains for a constant false-alarm rate (CFAR) incoherent narrowband processor. We investigate both parametric locally optimum and nonparametric filtering of the time-domain data to enhance weak signal detection. Simulated Rayleigh fading signals were inserted into the noise data, and the detection threshold was found to be lowered by about 4 dB over conventional processing, for signal frequencies 1.5 kHz and 4.5 kHz and a false-alarm probability of 0.0001. Performance degradations can potentially occur at large signal-to-noise ratios, but these were mitigated using a simple technique for fusing the non-Gaussian processor with a conventional processor

RELEASE LIMITATION

Approved for public release

Published by

DSTO Systems Sciences Laboratory
PO Box 1500
Edinburgh South Australia 5111 Australia

Telephone: (08) 8259 5555
Fax: (08) 8259 6567

AR-012-483
October 2002

APPROVED FOR PUBLIC RELEASE

Sperm Whale Impulse Noise and Incoherent Narrowband CFAR Processing

Executive Summary

Ambient underwater acoustic noise is often dominated by sounds produced by marine creatures. Some of these noises are impulsive in character, and can seriously degrade sonar performance. This is the case with noise produced by sperm whales, which are commonly found in deep waters around the world. Impulsive noise is characterised by a high probability of occurrence of extreme data samples compared with "Gaussian" noise. The effect of intense, sustained impulsive interference on a conventional sonar is to severely degrade signal detection, and cause difficulties in selection of thresholds for automatic detection. This research was carried out under task DST 00/036, "Advanced Signal Processing for Passive Sonar." One component of this task is to investigate new processing techniques for improving sonar performance in the presence of biological noise interference.

The purpose of this report is two-fold. Firstly, we analyse the impulsive properties of sperm whale noise recorded in deep water off the coast of Manus Island, as a function of frequency band. The impulsive effects are particularly strong in the frequency range 1-6 kHz, and improvements to sonar performance can be expected within this range. We demonstrate this by measuring empirical gains for a sonar processor incorporating nonlinear filtering to improve weak signal detection, in a problem related to intercept detection of sonar pulses. We find that detection threshold (a processor performance metric corresponding to the signal-to-noise ratio (SNR) at the processor input required to give a probability of detection of 50% at a specified probability of false-alarm) is lowered by about 4 dB for signal frequencies of 1.5 kHz and 4.5 kHz and a false-alarm probability of 0.0001. The noise data used was obtained from a single hydrophone, but array data is required for future work so that gains on operational sonar systems can be established.

The second purpose of this report is to demonstrate a technique for mitigating against performance losses that can potentially occur at large SNRs. When multiple signals are present at large SNRs, nonlinear mixing effects at the nonlinear filter can lead to the generation of artefacts. The key is to develop a processing technique that eliminates problems at large SNRs, while retaining the weak signal gains. We propose a simple technique for fusing the nonlinear processor with a conventional processor, based on the application of a higher-order statistic of the received data as a switch between the two processors. We find that this is successfull in eliminating large SNR problems for data analysed to date.

Authors

Derek Bertilone
Maritime Operations Division

Derek Bertilone completed a BSc.(Hons) degree in Physics from the University of Western Australia in 1983, and graduated with a PhD from the Australian National University in 1988. From 1988 to 1998 he was first a Research Scientist and then Senior Research Scientist at DSTO Salisbury, where he carried out research into optical/infrared propagation, image modeling and statistical image processing. In 1998 he joined Maritime Operations Division at DSTO Stirling, to work on advanced signal processing techniques for passive sonar.

Damien Killeen
Maritime Operations Division

Damien Killeen joined Maritime Operations Division at DSTO Stirling in 1999, and works as a Professional Officer assisting in research into advanced signal processing for passive sonar. In 2001 he completed a BSc.(Hons) degree in Applied Physics from Curtin University of Technology.

Contents

1. INTRODUCTION 1

2. SPERM WHALE IMPULSE NOISE 2
   - 2.1 Data Set 2
   - 2.2 Kurtosis 3
   - 2.3 Envelope Distribution 4

3. INCOHERENT NARROWBAND CFAR 6
   - 3.1 Conventional Processor 6
   - 3.2 Non-Gaussian Processor 7
   - 3.3 Fused Processor 9
   - 3.4 Empirical Detection Gains 10
   - 3.5 Artefact Mitigation 12

4. CONCLUSIONS 16

5. ACKNOWLEDGEMENTS 16

6. REFERENCES 17

1. Introduction

Ambient underwater acoustic noise is often dominated by sounds produced by marine creatures. Some of these sounds are impulsive in character; the time-series of pressure values has a spikey appearance, with a higher probability of occurrence of extreme sample values than is the case for Gaussian noise. This is true for noise produced by snapping shrimp [1-2], and also for noise produced by sperm whales [3-7]. Snapping shrimp are found in warm, shallow waters, while sperm whales are common in deep waters around the world. It is important to understand the statistical properties of these noises. A conventional sonar processor is optimised to detect a signal buried in a background of Gaussian noise, and may perform poorly in the presence of intense and sustained impulsive noise interference. Signal detection may be significantly degraded, and difficulties can arise in the setting of thresholds for automatic detection. Improvements can be obtained by incorporating impulsive noise models into the design of the processor.

In this report we describe the frequency-dependent non-Gaussian properties of sperm whale noise recorded off the coast of Manus Island. We examine probability distributions for the noise, and their modelling using standard parametric distributions. Sonar processing can be improved by using nonlinear filtering techniques from non-Gaussian detection theory [8]. We demonstrate this by measuring the empirical gains for a constant false-alarm rate (CFAR) incoherent narrowband processor utilizing standard non-Gaussian techniques, in a problem related to intercept detection of continuous wave (CW) sonar pulses. We investigate nonlinear filtering of the time-domain data at the processor input to enhance weak signal detection, using both parametric locally optimum (LO) ([8, 9]) and nonparametric ([8, 10]) filters. The LO processor is adaptive; as each block of time-series data is read-in, the noise statistics are estimated from the data, noise model parameters are estimated, and the result used to tune the nonlinear filter to optimise the processor to detect weak signals buried in that data. Gains over conventional processing are measured for simulated Rayleigh fading signals inserted into the noise data.

When multiple signals are present, nonlinear filtering can potentially produce artefacts at the processor output at large SNRs, due to nonlinear mixing of the signals. This is a serious problem if not addressed, as it can cause confusion in signal classification. We suggest a simple technique for mitigating against this problem. As each segment of data is read-in, we estimate the marginal kurtosis and decide whether or not to apply nonlinear filtering. If the kurtosis is above a threshold then we apply the nonlinear filter, otherwise we process in the conventional way. Since the marginal kurtosis is lowered by the presence of strong narrowband signals, the processor reverts to a conventional processor when SNR becomes too large. This essentially fuses the outputs of the conventional and nonlinear processors using a simple 'or' rule. We have empirically chosen a threshold value which works well for our data, and make no attempt to optimise it here.

2. Sperm Whale Impulse Noise

2.1 Data Set

We use 33 minutes of data recorded off the coast of Manus Island, using a hydrophone located on the ocean bottom in water of depth 640 m.[1] The data is sampled at a rate of 32 kHz, and the system response is flat from about 50 Hz up to 10 kHz. Sperm whales were observed at the time of recording, and loud clicking and creaking sounds can be heard on audio, in a manner consistent with previously published studies ([3-7]). Fig. 1 shows the power spectrum; there is an intense artefact at 50 Hz, and several of its harmonics are also present. Sperm whales dominate the spectrum for frequencies between about 1 and 6 kHz.

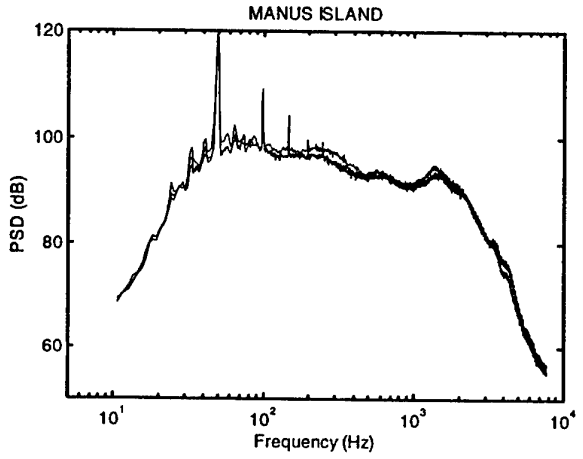

Figure 1. Power spectra. Averaged periodograms for 3 consecutive 5 minute segments of data. (Arbitrary reference level.)

The time-series often exhibits impulses arriving at regular time-intervals, as illustrated in Fig. 2. Individual whales tend to click at a regular rate of about 1-2 pulses per sec, and this can be observed in our data when a single whale dominates the noise. The rise and fall of the impulse amplitudes may be due to vocalisation directivity effects, as the whale turns towards the receiver and then away [5]. The background is dominated by clicking from other pod members. The data also exhibits occasional 'creaking' sounds,

[1] The analog recording was made in 1968, but was only recently digitised by D.Cato from DSTO Pyrmont.

believed to be clicking at a much higher rate and possibly associated with the whale diving for food [4].

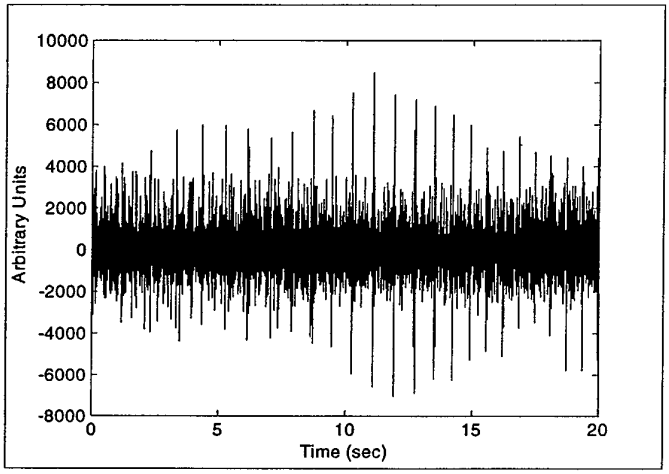

Figure 2. A time-series segment dominated by regular clicking from an individual whale.

2.2 Kurtosis

To characterise the non-Gaussian behaviour, we complex-demodulate the data in various passbands and compute the sample kurtosis of the in-phase and quadrature components. Kurtosis is the centralised fourth-order moment divided by the square of the variance. Gaussian noise has a kurtosis value of 3, while impulsive noise has a kurtosis greater than 3 provided the fourth-order moment exists. We use the deviation of kurtosis from the value 3 as a measure of non-Gaussian behaviour. We average the in-phase and quadrature kurtosis estimates; this gives an estimate of the kurtosis of the marginal probability density, assuming the joint density of the in-phase and quadrature components is circularly symmetric.

Fig. 3 shows a plot of the kurtosis in consecutive 500 Hz bands (0-500 Hz, 500-1000 Hz, etc.,) computed from 30 second segments of data that pass the K-S two-sample test of homogeneity.[2] Circles indicate the median of the kurtosis values obtained and error-bars indicate the 25-75 percentile range. The dashed line indicates the Gaussian value

[2] The Kolmogorov-Smirnov (K-S) two-sample test checks that the first-order probability distribution is homogeneous over the first and second halves of each data segment. We apply the test separately to the in-phase and quadrature components at the 5% significance level, and we consider the segment to pass the test only if both components pass. If the in-phase and quadrature components could be treated as independent (not strictly true for non-Gaussian noise, as the components at the same time instant may be uncorrelated but dependent [8-9]) then the overall level of the test would be 10%.

of 3. Kurtosis is particularly large in the frequency range 1-6 kHz, so non-Gaussian processing gains can be expected here. Maximum kurtosis occurs in the 4-4.5 kHz band.

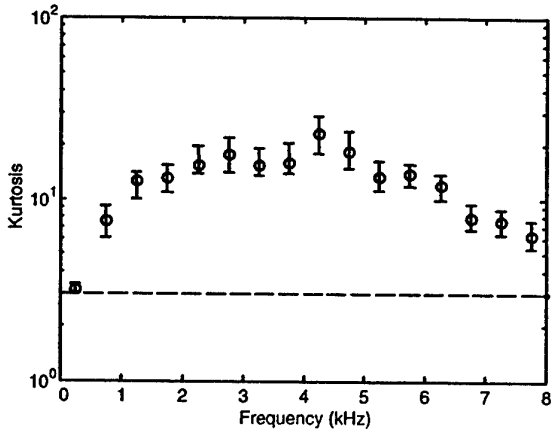

Figure 3. Kurtosis vs frequency (500 Hz bands). Average of in-phase and quadrature components.

2.3 Envelope Distribution

The exceedance probability is the probability that an envelope sample[3] exceeds a specified value. The triangle symbols in Fig. 4 show the empirical exceedance probability for a 30 sec segment of data in the 2-4 kHz band, that passed the K-S test of homogeneity. We note that the empirical distribution follows a continually bending curve on the log-log plot. Thus the distribution does not appear to exhibit a power-law fall-off, so an alpha-stable noise model [11] would appear to be inappropriate for this data.[4] Also shown are the predictions of several other impulsive noise models; the generalised Cauchy (GC) model ([9]), the Gaussian-Gaussian mixture (Mix) model ([12]), and the *K* model ([13]), with method of moments used to fit the models to the data.[5] Details of the envelope probability density functions (PDFs) are given in Table 1,

[3] The envelope sample at each time-instant is the square-root of the sum of the squares of the corresponding in-phase and quadrature samples.

[4] This is not surprising. Alpha-stable models arise from a generalised central limit theorem applicable in the limit of a large number of independent sources. In our case only a small number of whales dominates the data.

[5] We only consider a GC model with tail parameter $\nu > 2$, for which the second and fourth marginal moments exist.

and the relations used to apply method of moments are given in Table 2. Note that the moments refer to either the marginal data (in-phase and quadrature samples combined) or the envelope data.

None of the models gives a good fit over the full range of the data. The *K* model gives a good fit at large envelope values, but a poor fit at small envelopes. The Mix model also gives a good fit at large envelopes, but over a reduced range. The log-normal model (not shown) was found to give a good fit at small envelopes, but a poor fit at large envelope values.

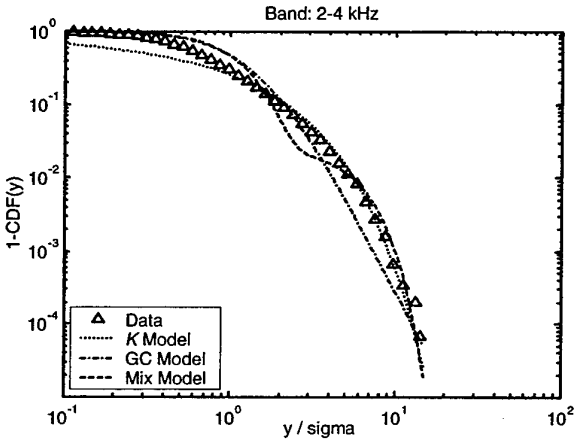

Figure 4. Envelope exceedance probability; empirical data and model predictions.

Table 1. Impulsive noise models; envelope PDFs and LO nonlinear filters.

	Envelope PDF; $p_0(y)$	*LO Nonlinear Filter;* $g(y)$
GC Model	$\frac{2\nu}{\beta^2} y \left(1+y^2/\beta^2\right)^{-\nu-1}$	$\frac{2(\nu+1)}{\beta^2}\left(1+y^2/\beta^2\right)^{-1}$
Mix Model	$\sum_{m=1}^{2} \frac{\varepsilon_m}{\sigma_m^2} y \exp(-y^2/2\sigma_m^2)$	$\frac{\sum_{m=1}^{2} \frac{\varepsilon_m}{\sigma_m^4} \exp(-y^2/2\sigma_m^2)}{\sum_{m=1}^{2} \frac{\varepsilon_m}{\sigma_m^2} \exp(-y^2/2\sigma_m^2)}$
K Model	$\frac{(y/\alpha)^{\lambda}}{2^{\lambda-1}\alpha\Gamma(\lambda)} K_{\lambda-1}(y/\alpha)$	$\frac{1}{\alpha y}\frac{K_{\lambda-2}(y/\alpha)}{K_{\lambda-1}(y/\alpha)}$

Table 2. Model parameters. Here m_2, m_4 and m_6 are the 2nd, 4th and 6th marginal moments, and e_2 and e_4 are the 2nd and 4th envelope moments.

	Noise Model Parameters from Moments
GC Model	$\beta^2 = \dfrac{2m_2 m_4}{m_4 - 3m_2^2}$ $\nu = \dfrac{2m_4 - 3m_2^2}{m_4 - 3m_2^2}$
Mix Model	$a = m_2^2 - m_4/3,\ b = m_6/15 - m_2 m_4/3,\ c = m_4^2/9 - m_2 m_6/15$ $\sigma_1^2 = \dfrac{-b + \sqrt{b^2 - 4ac}}{2a}$ $\sigma_2^2 = \dfrac{m_4/3 - m_2\sigma_1^2}{m_2 - \sigma_1^2}$ $\varepsilon_2 = \dfrac{m_2 - \sigma_1^2}{\sigma_2^2 - \sigma_1^2} = 1 - \varepsilon_1$
K Model	$\lambda = \dfrac{2e_2^2}{e_4 - 2e_2^2}$ $\alpha = \sqrt{\dfrac{e_2}{4\lambda}}$

3. Incoherent Narrowband CFAR

3.1 Conventional Processor

Non-Gaussian detection theory shows that nonlinear filtering can improve sonar performance in the presence of impulsive noise ([8-12]). We illustrate this point on a problem related to intercept detection of continuous wave (CW) pulses.[6] Our aim is to illustrate simple processing techniques that utilise the impulsive nature of the noise to improve performance, and is not intended to quantify the gains expected of any particular operational system. Our analysis uses data recorded from a single hydrophone, and can only hint at the gains that might be obtained using data from an intercept array on a sea-going platform.

[6] An intercept sonar is a passive sonar that detects pulse transmissions from the active sonar of an enemy vessel.

Conventional incoherent CW detection is based on FFTs. Each segment of complex-demodulated data,

$$\tilde{x}_n,\ n = 0,1,...,N-1$$

is tapered using a window function, w_n, a periodogram is computed, and a noise normalisation operator, F, is applied to equalise false-alarms across frequency (within each periodogram) and across time (between periodograms). The noise normalisation is to provide CFAR performance. The detection statistic for each FFT bin is given by the following,

$$\lambda(k) = F\left[\left|\sum_{n=0}^{N-1} w_n \tilde{x}_n \exp(-2\pi kn/N)\right|^2\right] \tag{1}$$

A widely used approach is for the operator F to run a sliding window across the periodogram, and divide each bin by the sample mean within that window. To avoid signal contamination, bins with extreme values are excluded from the estimate. We shall use the order-truncate-average algorithm ([14]) for this purpose,[7] and will refer to (1) as the "conventional processor." This will be our benchmark for performance. In practice the λ for several overlapping segments of data may be averaged, but in this study we will examine detection performance for individual periodograms. A detection is declared when the detection statistic exceeds a threshold, which is set to give a prescribed false-alarm rate.

3.2 Non-Gaussian Processor

Nonlinear filtering can be applied to enhance weak signal detection in impulsive noise ([8-12]). A nonlinear filter g is applied to the envelope of the time-series data, and its output used to re-scale each data sample. In the simplest case, g is a zero-memory filter with an output that is a decreasing function of the input, that acts to scale down the amplitude of extreme data samples. This reduces the spectral energy contributed to the periodogram by noise impulses, and enhances the detection of weak signals. Thus we replace (1) by,

$$\lambda'(k) = F\left[\left|\sum_{n=0}^{N-1} w_n g(|\tilde{x}_n|)\tilde{x}_n \exp(-2\pi kn/N)\right|^2\right] \tag{2}$$

[7] This is similar to a censored-mean CFAR processor, except that the number of bins rejected from the sample estimate of the mean is not fixed, but depends on the value of a parameter. We compute the median of all bins within the window, and reject bins with a value greater than the product of the median and the parameter.

We test several versions of the above, based on different choices of nonlinear filter. We include parametric locally optimum (LO) filters ([8-9]), and sub-optimal nonparametric filters ([8, 10]):

- *Parametric LO filters.* These are associated with optimum detection in the weak signal asymptotic limit.[8] The nonlinear function depends on $p_0(y)$, the envelope PDF under the noise-only hypothesis;

$$g(y) = -\frac{1}{p_0(y)} \frac{d}{dy}\left(\frac{p_0(y)}{y}\right) \tag{3}$$

- *Nonparametric filters.* These require no explicit knowledge of the noise PDF. An example is the hardlimiter narrowband correlator (HNC) filter ([8, 10]) which is widely used in impulsive environments;

$$g(y) = \frac{1}{y} \tag{4}$$

The parametric version of the processor requires a choice of noise model, and estimation of the model parameters from the received data. The LO filters for several impulsive noise models are given in Table 1. To apply the processor, we read-in a segment of time-series data, estimate the model parameters from that segment of data,[9] and then input these parameter estimates into the nonlinear filter to tune the processor. We then pass the same data segment through the processor according to (2). Our technique for estimating the model parameters is to apply method of moments directly to the received data, and assumes that the signal is sufficiently weak that its presence in the data has negligible effect on the moments. This means that the processor will perform poorly at large SNRs, due to signal contamination affecting the model parameter estimates. There is an additional factor which degrades performance at high SNRs; when multiple signals are present, nonlinear filtering mixes the signals to create artefacts (false signals) at other frequencies. This is a serious problem, as it creates confusion in signal classification. The nonparametric version of the processor uses the HNC filter, and also suffers from the artefact problem. The HNC processor requires no estimation of model parameters, but has the additional problem that it performs poorly in Gaussian noise ([10]). All of these problems are mitigated using a simple fusion technique described next.

---

[8] The LO filter arises in the problem of detecting a weak random-phase sinusoid in noise modelled as independent and identically distributed samples of a bivariate PDF with circular symmetry (see [8-9]).

[9] If the quantity of data is small, then we can combine with past segments to improve the parameter estimates. However this reduces the agility with which the processor adapts to changes in noise statistics.

3.3 Fused Processor

Our approach to mitigating against potential problems is to decide on a segment-by-segment basis whether or not to apply nonlinear filtering. As each segment of data is read-in, we estimate the marginal kurtosis of the data; i.e., the kurtosis of the in-phase and quadrature samples.[10] This will correspond to the marginal kurtosis of the background impulsive noise when SNR is small, but will reduce in value as SNR increases. For example, if one or more Rayleigh fading signals are present in the data, then the marginal kurtosis will drop to a value of 3 as SNR becomes large. We use the kurtosis as an indicator of the presence of strong signals, and to switch between Gaussian and non-Gaussian processing. If the kurtosis estimate is larger than a threshold value then we apply the nonlinear filter, otherwise we process that data segment in the conventional manner. In effect, this fuses the output of the non-Gaussian processor with the output of a conventional processor, using a simple 'or' fusion rule.[11] We have found this procedure to be effective in eliminating degradations at large SNRs, for both parametric and nonparametric processors, while maintaining gains over conventional processing at small SNRs. In addition, this technique ensures that the nonparametric HNC processor reverts to a conventional processor when the noise environment ceases to be impulsive.

Suppose the complex demodulated data comprises one or more independent signals added to background noise. Let x denote either the in-phase or quadrature component, and K_x its corresponding kurtosis. Noting that $x=s+n$, where s denotes signal with kurtosis K_s, and n denotes noise with kurtosis K_n, it follows after expansion of the moments in K_x that,

$$K_x = \frac{K_n + 6r + K_s r^2}{(1+r)^2} \tag{5}$$

$$r = \frac{< s^2 >}{< n^2 >} = \sum_m \frac{< s_m^2 >}{< n^2 >} \tag{6}$$

where s_m is the m^{th} signal. For the case of Rayleigh fading narrowband signals, K_s=3 and (5) reduces to,

$$(K_x - 3) = \frac{(K_n - 3)}{(1+r)^2} \tag{7}$$

---

[10] This could be done by computing the sample kurtosis of the in-phase and quadrature components separately, and then averaging. An alternative approach, which is used in this study, is to combine the in-phase and quadrature data and compute the sample kurtosis of this extended data set.

[11] As a precaution, the mixture model processor also switches to conventional processing if the estimate of one of the variances of the Gaussian components is negative.

Equation (7) shows that a kurtosis threshold can be chosen to ensure that the processor reverts to conventional processing when SNR exceeds any value at which significant degradations appear. Ideally, the threshold should depend on the background noise itself; a highly impulsive noise might require a higher threshold than a moderately impulsive noise.[12] Alternatively, one might choose a constant threshold and plan for a worse case scenario. In this case a particularly high threshold might be used, which will reduce the risk of any degradation occurring, but will also reduce the weak signal gains over conventional processing in moderately impulsive noise. In the current study we have chosen the kurtosis thresholds on an ad-hoc basis, and have made little effort to optimise their values. Nevertheless, promising results have been obtained. Unless otherwise stated, all processors (parametric and nonparametric) use a kurtosis threshold value of 5.

3.4 Empirical Detection Gains

We measure the empirical gains for detecting Rayleigh fading CW signals inserted into the noise data. We insert the signal into a large number of test data segments, and run the processors on each segment. We empirically determine the threshold required to give a specified fraction of false-alarms (P_f) in bins excluding windows around the signal bin and near the band edges. We then measure the fraction of detections (P_d) at this false-alarm rate, by counting the fraction of segments for which the empirical threshold is exceeded by the largest bin in a small window centred on the signal frequency. We repeat for various SNRs,

$$SNR = 10\log_{10}\left(\frac{N < a^2 >}{< n_I^2 + n_Q^2 >}\right) \tag{8}$$

to give a plot of the fraction of detections vs SNR. In (8) N is the FFT length, $<a^2>$ is the mean-squared signal amplitude, and $<n_I^2>$ and $<n_Q^2>$ are the mean-square of the in-phase and quadrature noise samples. The latter are estimated from the test data before the signal is added.

Fig. 5 shows results for detection of (a) a 1.5 kHz signal in a 1-2 kHz passband, and (b) a 4.5 kHz signal in a 4-8 kHz passband. In both cases the pulse-width was matched to the FFT length. In (a) the pulse-width was 2 secs, FFT length was 2048 samples, and 800 periodograms were tested. In (b) the pulse-width was 250 millisec, FFT length was 1024 samples, and 1600 periodograms were tested. In both cases, the false-alarm probability was 0.0001, and over 1.25 million noise-only bins were used to empirically establish the thresholds. The results indicate a **4 dB** gain for non-Gaussian processing over conventional processing, measured in terms of the reduction in detection threshold.

[12] This is complicated by the fact that the SNR at which degradations appear might itself depend on the kurtosis of the noise.

(Detection threshold is the SNR required to give a P_d of 50% at a given P_f, in this case P_f=0.0001). All versions of the non-Gaussian processor performed equally well, with only marginal differences in gain.[13]

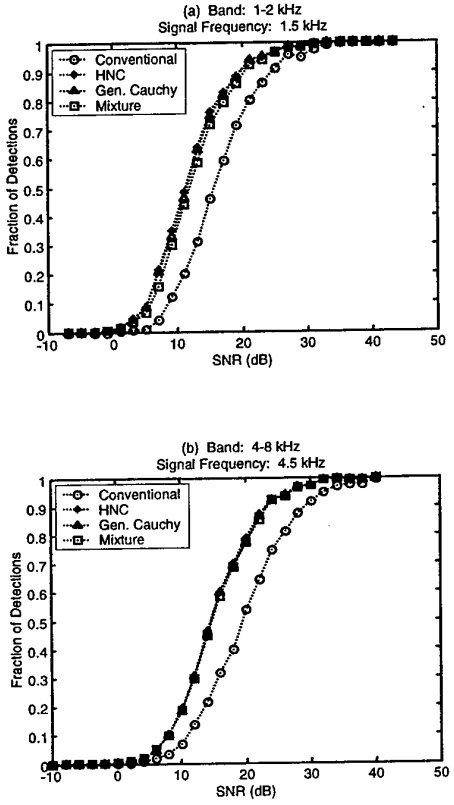

Figure 5. Probability of detection vs SNR (P_f= 0.0001). (a) 1-2 kHz band, f_s=1.5 kHz, (b) 4-8 kHz band, f_s=4.5 kHz.

The fusion technique based on kurtosis thresholding was successful in eliminating degradations in the parametric processors, associated with signal contamination affecting the model parameter estimates at large SNRs. A comparison with results obtained by running the processors in a manner that used noise-only data to estimate the model parameters, revealed no significant loss in weak signal gain. It also eliminated problems arising from the received data having a light-tailed distribution (i.e., kurtosis less than the Gaussian value of 3). In such cases, the nonparametric HNC

[13] An exception is the processor based on the *K* model, which gave significantly worse performance and has not been included in Fig. 5. The reason for the poor performance is unclear, and is a matter for further investigation.

processor gives poorer detection performance than a conventional processor ([10]), while the parametric processors based on impulsive noise models can fail, causing "drop-outs" in signal detection. In the next Section we show that the fusion technique also solves the artefact problem.

3.5 Artefact Mitigation

The artefact problem is caused by nonlinear mixing when multiple signals are present at large SNRs, and leads to the appearance of false signals at new frequencies.[14] This is illustrated in Fig. 6. This shows the outputs of each processor when applied to consecutive segments of data in the 2-4 kHz band, when fusion with a conventional processor is not applied. Two Rayleigh fading signals were inserted into each data segment (at frequencies of 2.5 kHz and 2.8 kHz) with the same SNR, and the SNR was increased from segment to segment. The images in the figure show pixel colour corresponding to the value of the detection statistic, plotted as functions of time and frequency, but with SNR used to label the time-axis (since SNR is linearly related to time). The image at top left is for a conventional processor. The other images are for non-Gaussian processors, and show the generation of a cascade of false signals, which first appear for an SNR in the range 30-40 dB, and which grow in number as SNR increases.[15] By comparison, Fig. 7 shows the same as Fig. 6, but with fusion applied, and demonstrates the elimination of artefacts.

One can devise a more sensitive test of the ability of the fusion technique to eliminate artefacts. We measure the probability of detecting a given signal vs SNR, when several other signals with the same SNR are also present in the data. We keep the probability of false-alarm fixed, but we include artefacts in the false-alarm count. We exclude from the false-alarm count, (i) a window of bins around all signals, and (ii) a widow of bins near the band edges, but we include bins containing artefacts. Fig. 8 shows results for detecting a 1.5 kHz signal in the 1-2 kHz band, with P_f=0.0001. Other signals are present in the data at (a) 1.625 kHz, (b) 1.625 kHz and 1.375 kHz, and (c) 1.625 kHz, 1.375 kHz, 1.25 kHz and 1.75 kHz. Comparing with Fig. 5(a), it can be seen that there is no significant loss of weak signal detection performance, and no degradation at high SNRs (except for a marginal degradation of the fused HNC processor, evidenced by a slight dip in P_d).

---

[14] Strictly speaking, the artefact problem will arise whenever the product of the data sample with $g(y)$ is a nonlinear function of the data sample. Thus it is only avoided when the filter g is a constant.

[15] Several other points can be noted from Figs. 6-7. Firstly, the difference in SNR at which the two signals first appear is due to spectral variation within the passband; the nominal SNR, as defined by (8), is the same for both signals, but the true SNR is larger for the 2.8 kHz signal than for the 2.5 kHz signal. Secondly, the horizontal striping observed in the parametric processor outputs in Fig. 6, is the "drop-out" effect associated with processor failure, as discussed in Section 3.4.

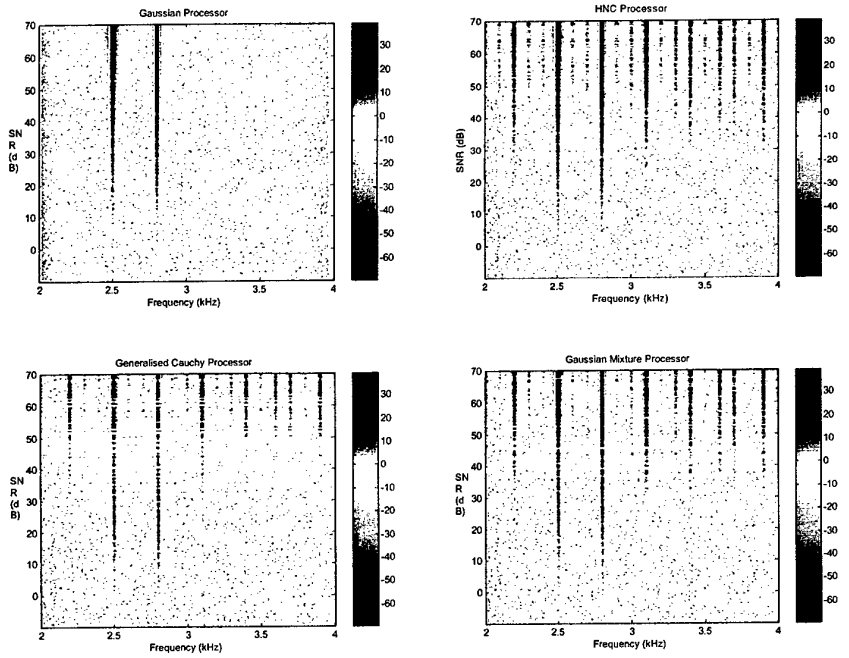

Figure 6. Non-Gaussian processors without fusion.

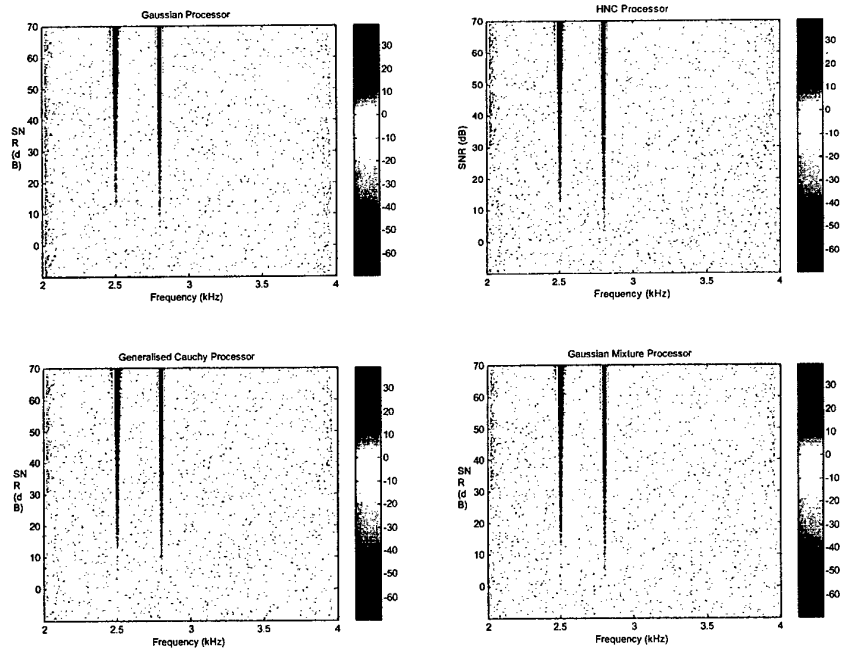

Figure 7. Non-Gaussian processors with fusion.

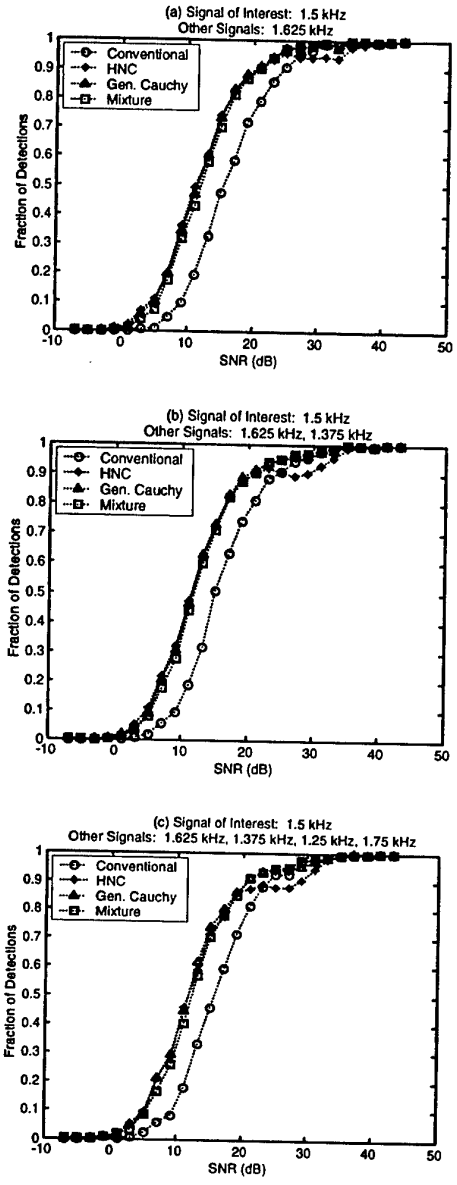

Figure 8. P_d vs SNR (P_f= 0.0001) for a 1.5 kHz signal. The passband contains (a) one, (b) two and (c) four other signals at the same SNR. Artefacts are counted as false-alarms.

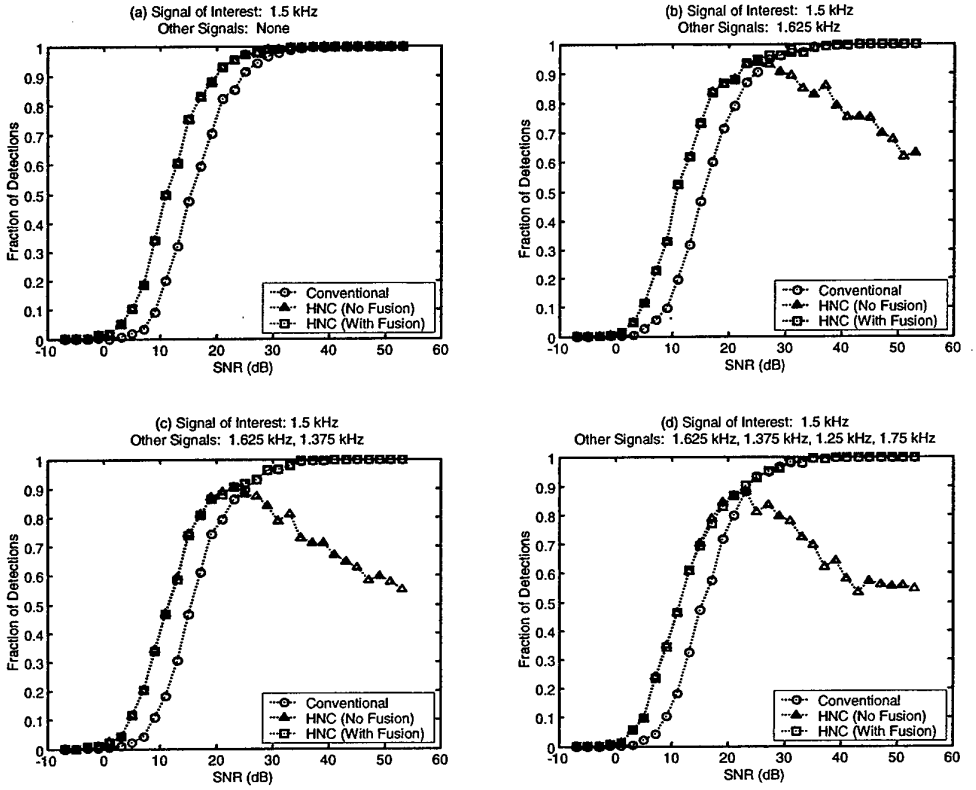

Figure 9. P_d vs SNR (P_f= 0.0001) for a 1.5 kHz signal, using a larger kurtosis threshold for the fusion than in Figs. 5-8. The passband contains (a) none, (b) one, (c) two and (d) four other signals at the same SNR. Artefacts are counted as false-alarms.

The slight degradation for the fused HNC processor is due to the fact that the chosen kurtosis threshold was a little too low (a value of 5 was used for all fused non-Gaussian processors in Figs. 5-8), and disappears when the kurtosis threshold is increased. This is illustrated in Fig. 9, which shows P_d vs SNR for the same multiple signal scenario as before, but this time using a higher kurtosis threshold value of 9. In this case the fused HNC processor shows no dip in P_d at large SNRs, while the low SNR detection performance is unchanged. For comparison, the figure also shows the corresponding results for a HNC processor without fusion, to demonstrate the severe degradation that occurs at high SNRs, as artefacts are generated in increasing numbers and counted as false-alarms.

4. Conclusions

Sonar performance is degraded in the presence of impulsive noise interference. Some of the performance loss can be regained using nonlinear filtering techniques from non-Gaussian detection theory. Improvements in detection threshold of 4 dB were obtained in this study, for CFAR incoherent narrowband detection in noise dominated by sperm whale clicking. The noise data used was obtained from a single hydrophone, but array data is required for future work so that the gains on operational sonar systems can be established. The key to practical implementation of non-Gaussian processing techniques is to make the processor robust to deviations from the assumptions underlying the processor design.

In principle, problems can occur when multiple signals are present at large SNR, due to generation of false signals from nonlinear mixing effects. This problem arises for both parametric and nonparametric processors. Parametric processors have additional problems associated with the estimation of model parameters when only signal+noise data is available. The nonparametric HNC processor also has the problem of requiring the noise environment to be sufficiently impulsive before gains over conventional processing can be obtained.

In this report we have examined a technique for overcoming these problems; the marginal kurtosis of the received data is used as a switch between linear and nonlinear filtering. This effectively fuses the non-Gaussian and conventional processor outputs on a segment-by-segment basis. This technique has shown promise in eliminating degradations in data analysed to date, but further work is required before the robustness of the technique can be established. In particular, the issue of selecting a kurtosis threshold requires more study.

5. Acknowledgements

We thank Dr. Doug Cato from DSTO Pyrmont for providing us with the digitised sperm whale data.

6. References

1. F.A.Everest, R.W.Young and M.W.Johnson, "Acoustical characteristics of noise produced by snapping shrimp," J. Acoust. Soc. Am. **20**, 137-142 (1948).

2. D.H.Cato and M.J.Bell, "Ultrasonic ambient noise in Australian shallow waters at frequencies up to 200 kHz," DSTO report, MRL-TR-91-23 (1992).

3. W.A.Watkins and W.E.Schevill, "Sperm whale codas," J. Acoust. Soc. Am. **62**, 1485-11490 (1977).

4. J.C.Goold and S.E.Jones, "Time and frequency domain characteristics of sperm whale clicks," J. Acoust. Soc. Am. **98**, 1279-1291 (1995).

5. B.Mohl, M.Wahlberg, P.T.Madsen, L.A.Miller and A.Surlykke, "Sperm whale clicks: Directionality and source level revisited," J. Acoust. Soc. Am. **107**, 638-648 (2000).

6. G.Pavan, T.J.Hayward, J.F.Borsani, M.Priano, M.Manghi, C.Fossati and J. Gordon, "Time patterns of sperm whale codas recorded in the Mediterranean sea 1985-1995," J. Acoust. Soc. Am. **107**, 3487-3495 (2000).

7. N.Jaquet, S.Dawson and L.Douglas, "Vocal behavior of sperm whales: Why do they click," J. Acoust. Soc. Am. **109**, 2254-2259 (2001).

8. S.A.Kassam, *Signal Detection in Non-Gaussian noise*. Springer-Verlag (1988).

9. N.H.Lu and B.A.Eisenstein, "Detection of weak signals in non-Gaussian noise," IEEE Trans. Information Theory, **IT-27**, 755-771 (1981).

10. S.A.Kassam, "Nonparametric hard limiting and sign detection for narrowband deterministic and random signals," IEEE J. Oceanic Eng., **OE-12**, 66-74 (1987).

11. C.L.Nikias and M.Shao, *Signal Processing with Alpha-Stable Distributions and Applications*. John Wiley and Sons, Inc., (1995).

12. D.W.J.Stein, "Detection of random signals in Gaussian mixture noise," IEEE Trans. Information Theory, **IT-41**, 1788-1801 (1995).

13. E.Jakeman and P.N.Pusey, "Significance of K distributions in scattering experiments," Phys. Rev. Lett., vol. **40**, 546-550 (1978).

14. R.O.Nielsen, *Sonar Signal Processing*. Artech House (1991).

DISTRIBUTION LIST

Sperm Whale Impulse Noise and
Incoherent Narrowband CFAR Processing

Derek Bertilone and Damien Killeen

AUSTRALIA

DEFENCE ORGANISATION

Task Sponsor **Chief, Maritime Operations Division**

S&T Program

Chief Defence Scientist
FAS Science Policy
AS Science Corporate Management
Director General Science Policy Development
} shared copy

Counsellor Defence Science, London (Doc Data Sheet)
Counsellor Defence Science, Washington (Doc Data Sheet)
Scientific Adviser to MRDC Thailand (Doc Data Sheet)
Scientific Adviser Joint
Navy Scientific Adviser
Scientific Adviser - Army (Doc Data Sheet and distribution list only)
Air Force Scientific Adviser
Director Trials

Systems Sciences Laboratory

Research Leader, Submarine Operations, MOD
Research Leader, Maritime Sensor Systems, MOD
Head, Submarine Sonar, MOD
Head, Sonar Processing and Systems, MOD
Head, Shallow Water Environment, MOD
Head, High Frequency Sonar, MOD
Head, Underwater Acoustics and Ocean Measurements, MOD
Dr. Derek Bertilone, MOD (2 copies)
Mr. Damien Killeen, MOD
Dr. Jane Perkins, MOD
Dr. Daniel Solomon, MOD
Dr. Andrew Knight, MOD
Dr. Mike Greening, MOD
Dr. Scott Foster, MOD
Mr David Bartel, MOD

DSTO Library and Archives

Library Edinburgh 1 copy
Australian Archives
Library, Stirling

Capability Systems Staff
Director General Maritime Development
Director General Land Development
Director General Aerospace Development (Doc Data Sheet only)

Knowledge Staff
Director General Command, Control, Communications and Computers (DGC4) (Doc Data Sheet only)

Navy
SO (SCIENCE), COMAUSNAVSURFGRP, NSW (Doc Data Sheet and distribution list only)

Army
ABCA National Standardisation Officer, Land Warfare Development Sector, Puckapunyal (4 copies)
SO (Science), Deployable Joint Force Headquarters (DJFHQ) (L), Enoggera QLD (Doc Data Sheet only)

Intelligence Program
DGSTA Defence Intelligence Organisation
Manager, Information Centre, Defence Intelligence Organisation

Defence Libraries
Library Manager, DLS-Canberra
Library Manager, DLS - Sydney West (Doc Data Sheet Only)

UNIVERSITIES AND COLLEGES
Australian Defence Force Academy
Library
Head of Aerospace and Mechanical Engineering
Serials Section (M list), Deakin University Library, Geelong, VIC
Hargrave Library, Monash University (Doc Data Sheet only)
Librarian, Flinders University

OTHER ORGANISATIONS
National Library of Australia
NASA (Canberra)

OUTSIDE AUSTRALIA

INTERNATIONAL DEFENCE INFORMATION CENTRES
US Defense Technical Information Center, 2 copies
UK Defence Research Information Centre, 2 copies
Canada Defence Scientific Information Service, 1 copy
NZ Defence Information Centre, 1 copy

ABSTRACTING AND INFORMATION ORGANISATIONS
Library, Chemical Abstracts Reference Service
Engineering Societies Library, US
Materials Information, Cambridge Scientific Abstracts, US

Documents Librarian, The Center for Research Libraries, US

INFORMATION EXCHANGE AGREEMENT PARTNERS

Acquisitions Unit, Science Reference and Information Service, UK
Library - Exchange Desk, National Institute of Standards and Technology, US

SPARES (5 copies)

Total number of copies: **57**

DEFENCE SCIENCE AND TECHNOLOGY ORGANISATION
DOCUMENT CONTROL DATA

1. PRIVACY MARKING/CAVEAT (OF DOCUMENT)

2. TITLE

Sperm Whale Impulse Noise and Incoherent Narrowband CFAR Processing

3. SECURITY CLASSIFICATION (FOR UNCLASSIFIED REPORTS THAT ARE LIMITED RELEASE USE (L) NEXT TO DOCUMENT CLASSIFICATION)

Document	(U)
Title	(U)
Abstract	(U)

4. AUTHOR(S)

Derek Bertilone and Damien Killeen

5. CORPORATE AUTHOR

Systems Sciences Laboratory
PO Box 1500
Edinburgh South Australia 5111 Australia

6a. DSTO NUMBER	6b. AR NUMBER	6c. TYPE OF REPORT	7. DOCUMENT DATE
DSTO-TR-1357	AR-012-483	Technical Report	October, 2002

8. FILE NUMBER	9. TASK NUMBER	10. TASK SPONSOR	11. NO. OF PAGES	12. NO. OF REFERENCES
M9505/21/0177	DST 00/036	CMOD	17	14

13. URL on the World Wide Web

http://www.dsto.defence.gov.au/corporate/reports/DSTO-TR-1357.pdf

14. RELEASE AUTHORITY

Chief, Maritime Operations Division

15. SECONDARY RELEASE STATEMENT OF THIS DOCUMENT

Approved for public release

OVERSEAS ENQUIRIES OUTSIDE STATED LIMITATIONS SHOULD BE REFERRED THROUGH DOCUMENT EXCHANGE, PO BOX 1500, EDINBURGH, SA 5111

16. DELIBERATE ANNOUNCEMENT

No Limitations

17. CITATION IN OTHER DOCUMENTS Yes

18. DEFTEST DESCRIPTORS

Sonar detection, Signal processing, Marine biological noise.

19. ABSTRACT

Impulsive noise interference of a biological origin is common in underwater acoustic environments. Here we report on properties of impulsive noise produced by sperm whales, recorded in deep water off the coast of Manus Island. We analyse the noise as a function of frequency band, and find strong non-Gaussian effects in the range 1-6 kHz. Sonar performance can be improved by utilising nonlinear filtering techniques from non-Gaussian detection theory. We demonstrate this by measuring empirical gains for a constant false-alarm rate (CFAR) incoherent narrowband processor. We investigate both parametric locally optimum and nonparametric filtering of the time-domain data to enhance weak signal detection. Simulated Rayleigh fading signals were inserted into the noise data, and the detection threshold was found to be lowered by about 4 dB over conventional processing, for signal frequencies 1.5 kHz and 4.5 kHz and a false-alarm probability of 0.0001. Performance degradations can potentially occur at large signal-to-noise ratios, but these were mitigated using a simple technique for fusing the non-Gaussian processor with a conventional processor